The 2009 IEEE/RSJ International Conference on
Intelligent Robots and Systems
October 11-15, 2009 St. Louis, USA

An Assistive Mask with Biorobotic Control to Enhance Facial Expressiveness

Dushyantha Jayatilake, *Student Member*, IEEE, Keisuke Takahashi, and Kenji Suzuki *Member*, IEEE

***Abstract*— This paper presents part of an on-going project to design a wearable supportive device, in particular for the facial paralyzed patients to enhance facial expressiveness. As various complications can result in facial disfigurement and loss of functionality in facial muscles it is required to develop a supporting device for people with such conditions. The previously proposed robot mask, which consists of a head supporter and motor units attempts to recreate facial expressions artificially by pulling the facial skin through cables attached to the skin. Since a facial expression is the result of the full or partial activation of combination of facial muscles, it is necessary to control the amount of displacement of the artificially created skin movement. Furthermore, in order to facilitate interpersonal timing of facial expressions, it is necessary to be able to read the nerve signals and process them in real time. This paper presents a compact and fully controllable actuation unit for the earlier proposed robot mask, and analyzes the relationship between the displacement of the specifically selected areas of the face and the actuation by control unit. It also present a bioelectrical signal based real time signal processing system to determine the requirement for an artificial expression.**

***Index Terms*— Robot Assisted Mask, Wearable Robot, Facial Expressiveness, Bioelectrical Signals, Silent Actuation**

I. INTRODUCTION

Facial expressions, one of the most effective means of expression based non-verbal communication, and often understood universally, assumes a significant part in social information exchange. The six different facial expressions: happiness, sadness, fear surprise, disgust, and anger are typically identified by the psychologists as basic facial expressions [1], and Batty et. at 2003 [2] reported that humans have a very fast processing speed in identifying these six expressions. They also noted that positive expressions such as happy and surprise are identified even faster than the negative expressions such as sadness and disgust.

Various complications can make a face less responsive. Facial paralysis: the total or partial loss of voluntary muscle movement, which is fairly common than many may think [3], can cause severe distraction in many ways. Physically, it makes the person less responsive while resulting in difficulties in eating, drinking and talking etc. due to the inability to purse the lips tightly. It can also cause tearing disorders, and the inability to blink or close the eyelid completely makes the cornea of the eye vulnerable to dryness [4]. The loss of baseline muscle tone in hemifacial paralysis course changes in facial appearance, such as drooping of the ipsilateral face and and deviation of the nose to the contralateral side of the face [5]. This facial disfigurement can result in social and vocational handicap which could eventually lead to social isolation.

Earlier we presented the design of a robotic mask with Shape Memory Alloy (SMA) based actuators, that can be used as a supportive tool to emulate the facial expressive function [3], [6]. The approach we proposed was to create artificial facial expressions by pulling the anatomically selected points of the facial skin through wires attached to the skin. The SMA actuators basically work under the principle of thermal energy, hence they inherits some weakness during cooling, and due to its metallurgy it exhibits significant hysteresis in the strain-temperature, stress-strain and resistance-temperature relations [7], [8]. However, they posses the most important characteristic for the creation of facial expressions: the silent actuation. The silent actuation will essentially improve the quality of life of the user as it can perform similar to the natural sound-free expression process.

Ekman et.al (1970) indicated in their paper on Facial Action Coding System (FACS) [9], a facial expression is the result of the full or partial activation of combination of facial muscles. Therefore, in order to get natural looking expressions, it is necessary to control the amount of displacement of the artificially created skin movement. Although, facial expressions can be used to express emotional state of mind, they can also be used to facilitate the communication environment by modifying typical expressions in social situation to create the impression of culture-specific facial expressions of emotions. Despite the possibility of having extremely large number of expressions, when emotions are elicited only a limited number of them believed to be produced universally and discretely [10]. Ekman and Friesen in 1969 have noted that when an authority figure was present the Japanese more than the American masked negative expressions with the semblance of smile [11]. To facilitate such actions, the actuators need to have the capacity to control the amount of actuation continuously. As facial muscles are in charge of performing these expressions through the utilization of the signals of the facial nerve, any attempt to recreate facial expressions artificially will also required to equipped with a mechanism to recognize the expected activity of the facial muscle.

In this paper we mainly concentrate on the improved

This study was supported in part by the Global COE Program on "Cybernics: fusion of human, machine, and information systems" at the University of Tsukuba and also Grant-in-Aid, Yoshikawa-Ozawa Memorial Foundation for Electronics.

D. Jayatilake (dush@ai.iit.tsukuba.ac.jp), K. Takahashi (keisuke@ai.iit.tsukuba.ac.jp), and K. Suzuki (kenji@ieee.org) are with the Artificial Intelligence Laboratory of the Graduate School of Systems and Information Engineering, University of Tsukuba, Japan.

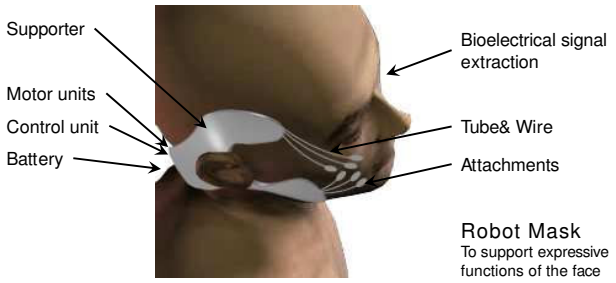

Fig. 1. The overview of the Non Invasive Robot Mask with six degrees of freedom of actuation

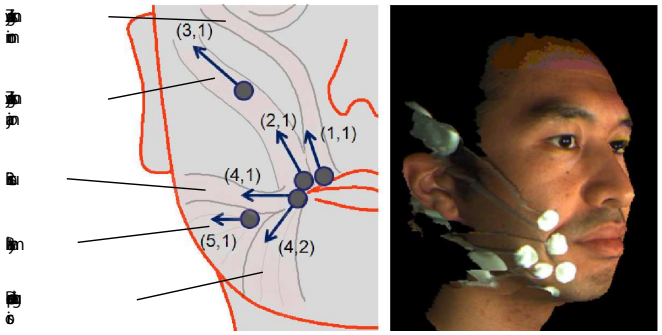

Fig. 2. Connection of pulling wires to the face. The figure to the left: Facial muscles, five pulling points, and the corresponding six pulling directions. The figure to the right: a 3D image of skin pulling.

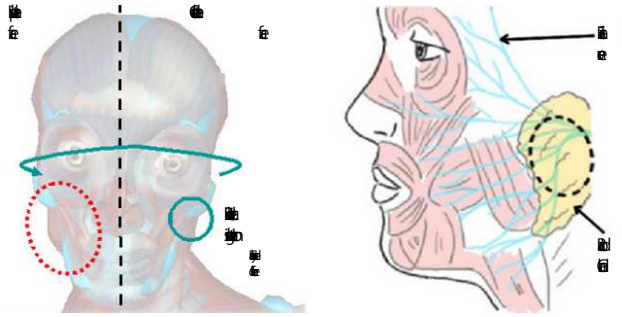

Fig. 3. Acquiring of bioelectrical signals near the parotid gland of the contralateral face

design of the earlier proposed actuator, the point to point controllability of the actuator by employing a "Discretized PID controller" and extension of the results to the skin displacement, and the utilization of the bioelectrical signals to achieve seamless control of the robot mask.

II. The Robot Mask

The robot mask (Fig. 1), which consists of a head supporter, motor unit and a pulling wire arrangement, attaches onto the face externally and pulls the facial skin through cables attached to the skin. The pulling motion is provided by the SMA based Silent Actuation (SIAC) units. They generate the skin displacement through the contraction and expansion of the SMA wires while operating without any mechanical noise. Each SIAC unit consist of a dedicated controller which facilitates the point to point feedback control of facial skin displacement.

The Robot mask which at present concentrates on hemifacial paralysis, consists of number of SIAC units and facilitates the movement of the ipsilateral face by the use of bioelectrical signals from the contralateral side of the face. This approach is based on the cross-facial nerve grafting technique, which is used to generate symmetrical facial expressions on hemifacial paralyzed patients. The human anatomy based selection of pulling points and the pulling directions, such that to closely emulate the movement of the six facial muscles responsible for the smile, as recognized by FACS: Zygomaticus major, Zygomaticus minor, Risorius, Platysma, and the Depressor anguli oris (Fig. 2), enhances the possibility of recreating natural looking artificial expressions. The bioelectrical signals mainly consisting of surface electromyographic (sEMG) signals are acquired not on the front of the face but near the Parotid Gland of the contralateral side (Fig. 3). Since the facial nerve passes through the Parotid Gland, this configuration will ensure the capturing of all the facial muscle signals of the ipsilateral face. This bioelectrical signal based brain interaction provides the seamless control of the robot mask while supporting the natural timing of facial message signs needed for interpersonal communication.

Fig. 2 shows the five pulling points with circles and the six pulling directions with arrows, and the six pulling actions are identified by their pulling points and the pulling directions respectively. Action 1 denoted by (1,1), actions 2 and 3 denoted by (2,1) and (3,1), action 4 denoted by (4,1), action 5 denoted by (5,1), and action 6 denoted by (4,2) are used to emulate the movement of Zygomaticus minor, Zygomaticus major, Risorius, Platysma, and Depressor anguli oris respectively.

III. Silent Actuation Unit

This can be considered as the heart of the Robot Mask system. Each artificial muscle unit has its own SIAC unit and all the SIAC units are located at the Back-Pack area of the robot mask. Earlier we presented the basic design for an SMA based linear actuator, using a helically wound Ni-Ti-Cu alloy based 0.15 [mm] diameter SMA wire with specific heat values of 6.1 [cal/mol°C] at martensite low-temperature phase to 8 [cal/mol°C] at austenite high-temperature phase to have a coil diameter of 0.62 [mm]. In this paper we present an enhanced version of the SIAC unit design, which facilitates point to point controllability with better stability. One major improvement of this design is the use of an incremental encoder to get the accurate and linear position feedback of the SMA wire contraction.

Fig. 4 shows the enhanced design of the Silent Actuation Unit (SIAC). Mainly it can be divided in to two sections as the sliding unit and the guiding exterior. Sliding unit is pulled by the SMA artificial muscle actuators connected at one end and it's other end is connected to skin pulling wires. Each actuator is made up of 2 to 3 artificial muscle wires in parallel. Since the hysteresis characteristics in SMA slows down its cooling rate [12],[13], springs are provided to accommodate quick return to original position during cooling.

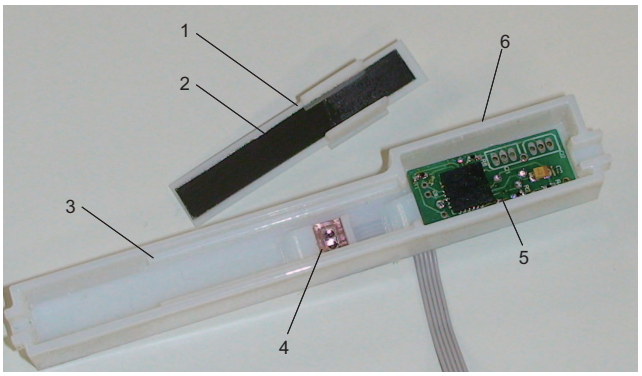

(a)

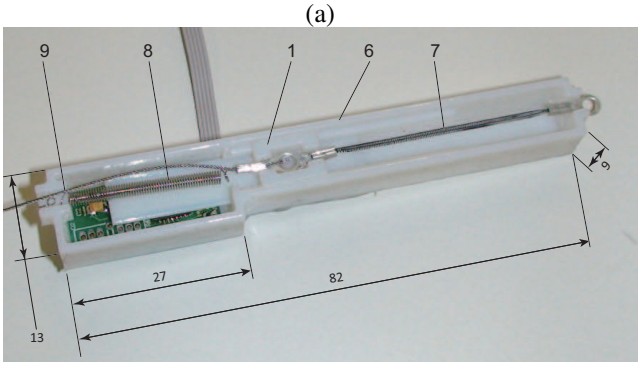

(b)

1	Slider	6	Outer
2	Encoder strip	7	SMA actuator
3	Slider guideway	8	Spring supporter
4	Reflective encoder	9	Pulling wire
5	Dedicated controller		

Fig. 4. Image of assembled SIAC unit with top (a) the encoder codestrip attached to the underside of the slider and bottom (b) the completely assembled SIAC unit which weights 8 [g] in total.

Wires are connected to the slider at the artificial muscle-spring junction of the slider and the encoder strip for the reflective type optical feed-back sensor (incremental encoder) is mounted at the bottom side of the slider (Fig. 4(a)). The dedicated controller implements the skin contraction control system. The SIAC outer provides the 36 [mm] long guideway and a cover for the slider. From outside it has the dimensions $9\times82\times13$ [mm] with 9 [mm] been the height of the unit.

Fig. 5 shows the block diagram of the operation inside the SIAC embedded control system (the slave controller). The controller which receives the actuation amount command through an I^2C communication channel, after querying with the Quadrature Encoder Interface (QEI) for the present position of the slider, adjusts the PWM duty ratio of MCPWM module at a sample rate of 100 [Hz].The resulting PWM duty ratio is sent to the Logic MOSFET driven voltage drive and the actuator (BMX) is driven directly from the PWM signal.

Fig. 6 shows the block diagram of the discretized PID controller based SIAC control system. The control system starts with the receiving of a actuation value through the I^2C communication channel. That value denoted here by X_{ref} represents a linear distance in millimeters. The feedback

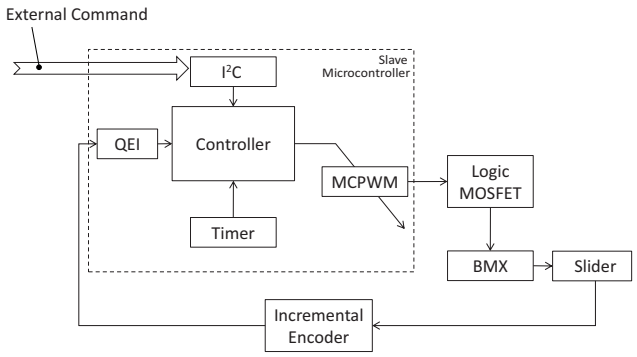

Fig. 5. Peripheral interfacing and module handling inside the slave system.

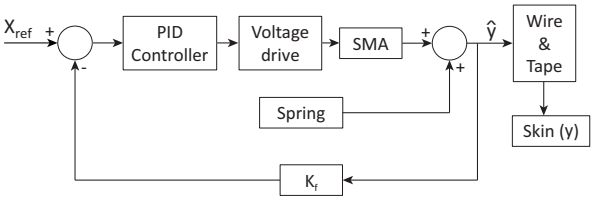

Fig. 6. The block diagram representation of the position control system.

sensor is a 150 [lines/inch] incremental encoder and the encoder interface (QEI of Fig. 5) has an interfacing logic of four counts per pulse, making it effectively 600 [counts/inch]. The feedback is taken at the slider, which is the SMA/Wire and tape junction, and with respect to position controlling, the quick return spring appears in a manner similar to a force disturbance.

A. Bioelectric Signal Based Control

The main target of bioelectrical signal based control is to obtain seamless control of artificially generated facial expressions and support the timing of facial message signs needed for interpersonal communication. By acquiring bio-electrical signals from the contralateral side of a hemifacial paralyzed patients and using them to actuate the artificial muscles of the ipsilateral side, we aim to artificially correct the baseline facial muscle tone, and minimize the drooping of the ipsilateral face. Fig. 7 shows the placement of Ag/AgCl surface EMG electrodes to capture bioelectrical signals of the Masseter muscle of the contralateral face. Fig. 8 shows the block diagram of the signal conditioning and processing unit used with these bioelectrical signals. A high pass filter (HPF) of 0.5 [Hz] was imposed on the amplified bioelectrical signal to remove DC noise, and in order to remove power line noise, a 50 [Hz] band eliminating filtering (BEF) was performed using a digital comb filter on the 300 [Hz], 8 bit analog to digital (A/D) converted signal (1). Then digital signal processing (DSP) was done on a 10 sample mooving window to obtain the actuator moving command.

$$C_k = S_{(k)} - S_{(k-\tau)} \tag{1}$$

where τ is an predetermined value, and $\tau = 6$ in this experiment.

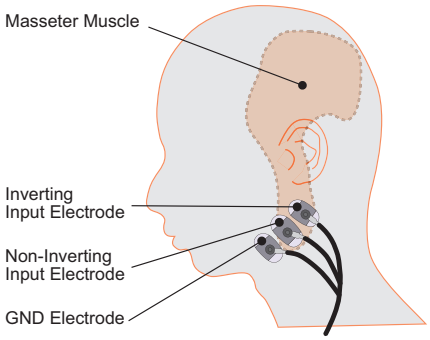

Fig. 7. Bioelectric signal capturing indicating the location of sEMG electrodes.

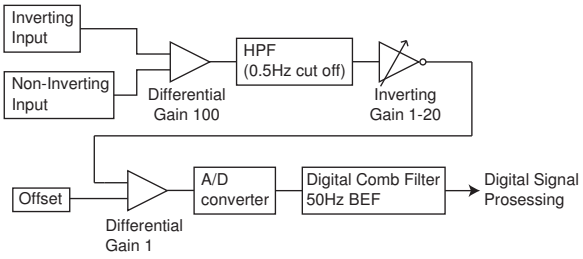

Fig. 8. Block-diagram view of the bioelectric signal acquisition and processing unit.

Fig. 9 shows the DSP criteria for establishing the actuation command, which is based on the real time integration and the variance of the digitally filtered signal. A threshold comparison of the 2 variables were used to assess the nature of the signal and 3 different mastication actions of *Relaxed*, *Semi-Stressed*, and *Stressed* were used to update in realtime the actuator displacement value issuing commands of *Remain*, *Increase*, and *Decrease*. The two actions, *Semi-Stressed* and *Stressed* were produced by the lite and tight gritting of teeth respectively.

B. Skin contraction and Sensor feedback

The control system of the Robot Mask uses an incremental type linear encoder with a resolution of 150 lines/inch. However as indicated by Fig. 6, the feedback measurement is taken at the slider and not on the face. When pulling from the outside there is a possibility of pulling wire slightly sinking into the face, and due to this there is a possibility of sensor not providing an accurate reading of the facial displacement. The actual displacement will also be affected by the characteristics of the skin-wire joint. Hence it is necessary to investigate how good an estimator $\hat{y}$ is for actual skin displacement: y. This scenario was analyzed through an offline comparison of the sensor data for point to point control with the findings of 3D image based actual skin displacements (Fig. 10) for all the artificial actuation actions: 1 to 6. This was done by capturing the pulling of the facial skin through a 3D scanner (NEC Danae100SP) and later comparing the actual skin displacement with the sensor observation.

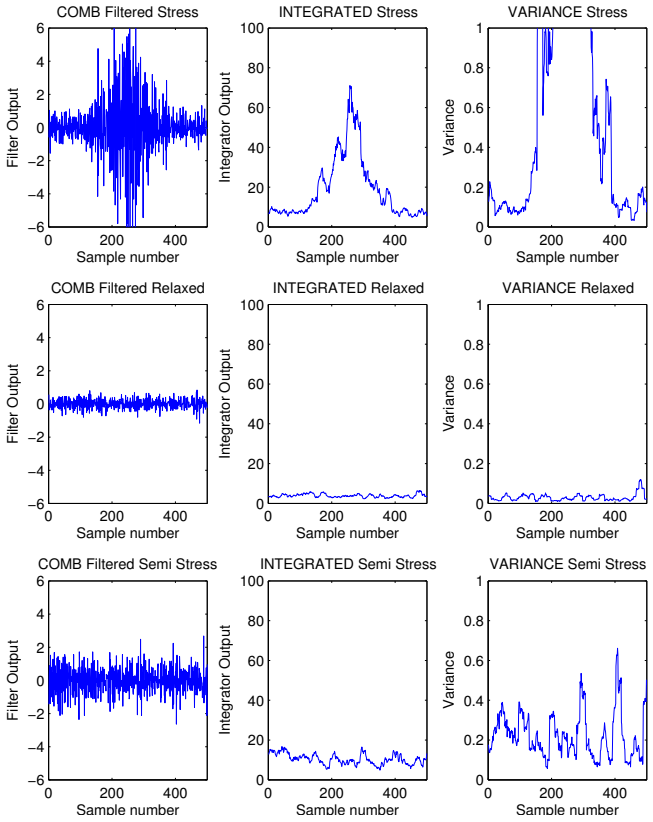

Fig. 9. The process of bioelectrical signal processing. The left most column: raw signal after Comb filtering: the middle column, integrated signal and the right most column: variance. The rows from top to bottom indicates the signal categories: Stressed, Neutral, and Semi-Stressed.

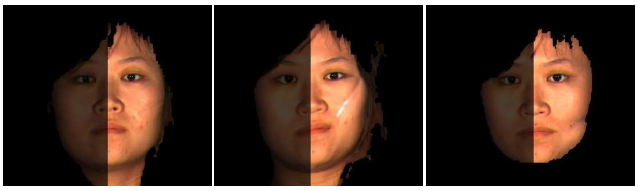

Fig. 10. Three dimensional photographs taken during artificial muscle simulations. Left: Neutral face, Center: Zygomaticus major simulation with a skin displacement of 6.6 [mm], and right: Risorius simulation with a skin displacement of 9.6 [mm].

IV. Results

Fig. 11 and Fig. 12 shows the controlling of the six artificial expression generating actions for the five pulling points. They show the tracking characteristics against the stepwise incrementing and decrementing values of the desired skin displacement. Data was acquired at a rate of 100 [Hz]. The Y axis shows the sensor indicated displacement value in [mm]. The results indicates good tracking characteristics for actuation amounts greater than 5 [mm], however the tracking is not so fluent for step down compared to step up.

Fig. 13 shows the step response for two step inputs of 5 [mm] and 10 [mm] respectively. In both the cases actuation started to occur at 1.75 [s] mark. The low step response exhibits higher oscillations, however the high step response performs well with oscillations less than ± 1 [mm].

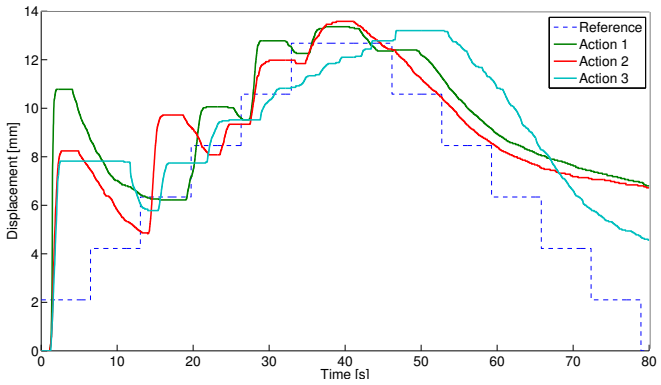

Fig. 11. Controllability of skin contraction of muscle actions 1, 2, and 3.

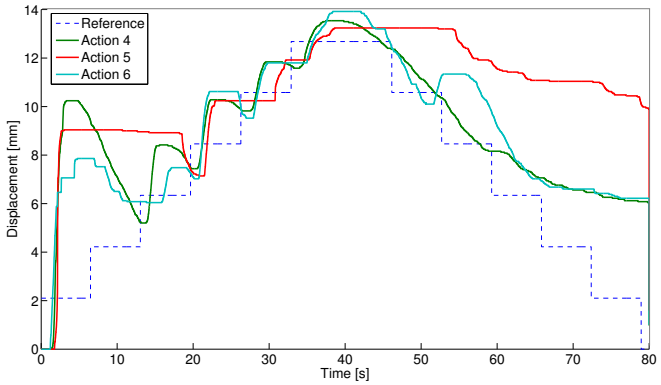

Fig. 12. Controllability of skin contraction of muscle actions 4, 5, and 6.

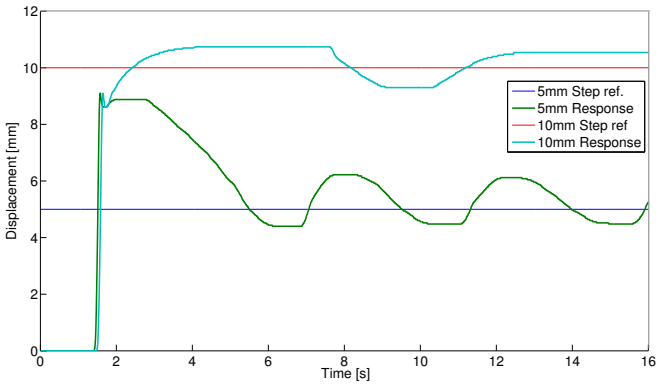

Fig. 13. Controller characteristics for two step inputs of 5mm and 10mm.

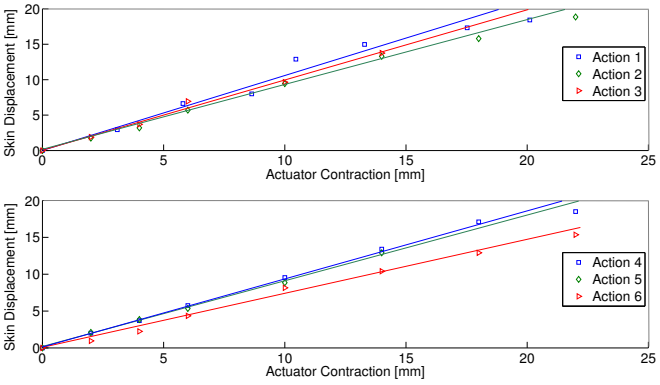

Fig. 14. Relation between the artificial muscle contraction and the actual skin displacement of a male subject.

Fig. 14 shows the actual skin displacement amounts against the corresponding sensor readings of a male subject for the six different artificial actuation configurations. All the displacement values are shown in millimeters. The results, as expected indicates slightly larger values for actuator contractions compared to their corresponding skin displacement values. By using a similar 3D scanner based technique it was also observed that pulling force of 160 [gf] on a female subject would result in a skin deviation of 12.2 [mm] along the zygomaticus major muscle direction and a deviation of 10.6 [mm] along the risorius muscle direction. Although a single test is not enough to determine the typical skin stiffness, it was used as a basic guideline for the establishment of SIAC requirements.

Fig. 15 shows the raw bioelectrical signal (the upper graph), the reference for displacement, and the actual displacement for a 110 [gf] constant load (the test was done with a fixed load and not on the face). The actual data was handled at a rate of 100 [Hz], however for better visibility only 1 in 20 points are shown in the X axis which corresponds to a appearance of 5 [Hz] sampling. The vertical dotted lines indicate the change of displacement control logic.

Performances

Fig. 16 shows the generation of expressions by using two actuators which emulate the muscles: zygomaticus major and risorius. Top left shows the neutral face, top right: 12 [mm] of actuation of both muscles, bottom left: 12 [mm] of actuation of zygomaticus major alone and bottom right: 6 [mm] of actuation of both muscles. By using 10 [μm] thick Polyurethane film type tapes, we were able to attach the transparent pulling wires to the skin with almost no visible disturbance. The experiment was conducted on a healthy female with no pre experimental skin preparations. In normal operation, the exterior and the interior of the SIAC has recorded average temperatures of about 37 [°C] and 44 [°C] respectively. Although at times the SMA wire reached as high as 97 [°C] , typically the high temperature state averaged around 68 [°C] (all the temperature data were recorded using a Chromel-Alumel K type thermocouple and a AND AD-5602 thermometer).

V. Discussion

Fig. 11 and Fig. 12 shows that actuator displacements are controllable and for displacements over 6 [mm] it is possible to control them with an error less than ± 1 [mm]. However, because of the high thermal inertia of SMA, at the beginning, they tend to have a starting delay of 1.5-2.0 [s] as well as a significant overshoot of the range of 350-500%. It would be possible to overcome this situation by maintaining a small duty ratio value at the PID channel all the time. However that would increase the power consumption hence a better solution would be to have an adaptive control system such

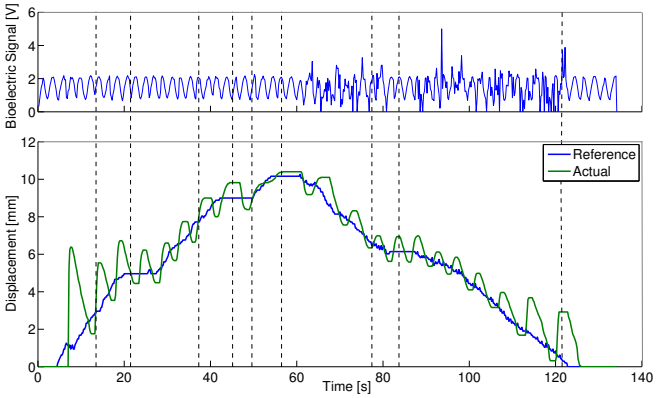

Fig. 15. The bioelectrical signal based skin displacement control for a constantly loaded actuator.

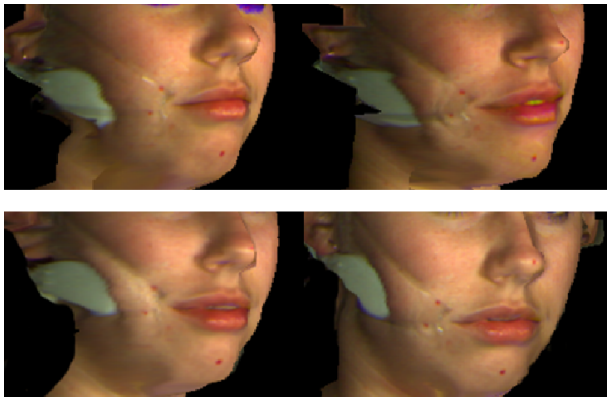

Fig. 16. Generation of facial expressions by using two actuators with feedback control.

that to heat up fast at the beginning and slowly later. Due to slow cooling, the stepping down action shows less accurate tracking characteristics compared to stepping up. In order to eliminate this it would be required to have an artificially controlled cooling system

Fig. 14 confirms that the slider displacement is a good enough estimator for the actual skin displacement. Also a second order polynomial approximation will results in difference as low as ± 1 [mm]. Fig. 15 shows an example of experimental results for bioelectrical signal based control. It shows the controllability of expressions as well as the possibility to use it in real time for seamless control of robot mask that can facilitate the interpersonal timing of each individual.

VI. CONCLUSIONS AND FUTURE WORKS

This paper has introduced an enhanced actuator, a position controller, and a bioelectrical signal based expression handler for the previously presented robot mask system. The new actuation system provides better stability and the incorporation of incremental encoder facilitates accurate feedback and better controllability. The compact and modular arrangement provides higher scalability which is required when expanding the mask functionality to the eye area of the face. The Discrete PID control system indicates the possibility of accurate position controlling, however given the high thermal inertia and hysteresis characteristics of SMA an adaptive control system likely to perform better. Nevertheless, the bioelectrical signal based control system described in this paper guaranties the feasibility of the previously proposed method.

One necessary addition to the SIAC unit is an artificial cooling system, and we expect to perform tests on a Peltier device based cooling system, and an adaptive control system to control both PWM duty ratio and the Peltier device simultaneously. Currently we are also investigating the possibility of using number of SMA wires in series for both pulling and return motion, and actuating only a limited number of them at a time so that some others can be used during the cooling of one set. The bioelectrical signal processing system presented in this paper, which is indeed based on the masseter muscle only determines the command for a single actuator, and we are now in the process of developing a facial nerve based signal processing algorithm to determine actuation amounts for each actuator.

REFERENCES

[1] N. Ahuja H. Wang. Facial expression decomposition. *Proc. of Ninth IEEE International Conference on Computer Vision (ICCV)*, Volume 2:pp. 958–965, Oct. 2003.

[2] Taylor M.J. Batty M. Early processing of the six basic facial emotional expressions. *Cognitive Brain Research*, 17(3):pp. 613–620, Oct. 2003.

[3] D. Jayatilake K. Suzuki A soft actuator based expressive mask for facial paralyzed patients. In *Proc. of 2008 IEEE/RSJ International Conference on Intelligent Robots and Systems*, pages 4048–4053, 2008. Nice, France.

[4] Barry M. Schaitkin Mark May. *Facial Paralysis: Rehabilitation Techniques*. Thieme, 2003.

[5] Myles L. Pensak. *Controversies in Otolaryngology*. Thieme, first edition edition, 2001.

[6] D. Jayatilake A. Gruebler and K. Suzuki. An analysis of facial morphology for the robot assisted smile recovery. In *Proc. of 4th IEEE International Conference on Information and Automation for Sustainability-ICIAFS.2008*, pages pp. 395–400, Dec. 2008. Colombo, Sri Lanka.

[7] Nagarajan T. Zoppi M. Sreekumar M., Singaperumal M. and Molfino R. Recent advances in nonlinear control technologies for shape memory alloy actuators. *Zhejiang University Press, Co-published with Springer-Verlag GmbH*, Volume 8:818–829, April 2007.

[8] C.L. Gu K. Yang. Modelling, simulation and experiments of novel planar bending embedded sma actuators. *Special Section of Revised Papers from the 8th International IFAC Symposium on Robot Control, 8th International IFAC Symposium on Robot Control, ScienceDirect*, Mechatronics Volume 18(Issue 7):323–329, September 2008.

[9] [Online] Available: `http://face-and-motion.com/dataface/general/homepage`.

[10] D. Matsumoto and B. Willingham. Spontaneous facial expressions of emotion of congenitally and noncongenitally blind individuals. *Personality and Social Psychology*, Vol. 96(No. 1):1–10, Jan. 2009.

[11] P Ekman. Facial expressions of emotion: an old controversy and new findings. *Philosophical Transactions of the Royal Society of London*, 335:pp. 63–69, 1992.

[12] R.A. Higgins. *Engineering Metallurgy*, volume Part 1: Applied Physical Metallurgy. Butterworth-Heinemann, 6 edition edition, 1993. pp. 402-403.

[13] C.L. Gu K. Yang. Modelling, simulation and experiments of novel planar bendign embedded sma actuators. *Elsevier*, Mechatronics(18):pp. 323–329, 2008.